Ordering in the SU(4)-symmetric model of AA bilayer graphene

A. V. Rozhkov, A. O. Sboychakov, and A. L. Rakhmanov
Institute for Theoretical and Applied Electrodynamics, Russian Academy of Sciences, 125412 Moscow, Russia

(Received 17 June 2023; revised 4 October 2023; accepted 6 November 2023; published 27 November 2023)

We examine possible ordered states of AA-stacked bilayer graphene arising due to electron-electron coupling. We show that under certain assumptions the Hamiltonian of the system possesses an SU(4) symmetry. The multicomponent order parameter is described by a 4×4 matrix $\hat{Q}$, for which a mean-field self-consistency equation is derived. This equation allows Hermitian and non-Hermitian solutions. Hermitian solutions can be grouped into three topologically distinct classes. First class corresponds to the charge density wave. Second class includes spin density wave, valley density wave, and spin-valley density wave. An ordered state in the third class is a combination of all the aforementioned density-wave types. For anti-Hermitian $\hat{Q}$ the ordered states are characterized by spontaneous interlayer loop currents flowing in the bilayer. Depending on the topological class of the solution these currents can carry charge, spin, valley, and spin-valley quanta. We also discuss the special case when matrix $\hat{Q}$ is not Hermitian and not anti-Hermitian. Utility and weak points of the proposed SU(4)-based classification scheme of the ordered states are analyzed.

DOI: 10.1103/PhysRevB.108.205153

I. INTRODUCTION

Discovery of series of alternating Mott insulating, metallic, and superconducting states in the magic-angle twisted graphene bilayer [1–3] was the first experimental evidence of the diversity of possible ordered states in bilayer graphene systems caused by electron-electron coupling. Recently, a cascade of transitions between different nonsuperconducting and superconducting states was observed in the well-researched [4–6] AB- (or Bernal) stacked bilayer graphene (AB-BLG). This feature is not limited to AB-BLG: the current studies (theoretical [7,8], numerical [9,10], and experimental [11]) indicate that even quite simple electronic systems may have several ordered states competing against each other to become the true ground state. The analysis of the cited above works shows that different ordered states of a specific model are close to each other in terms of their (free) energy. As a result, the true ground state of a system depends crucially on the experimental conditions (temperature, magnetic field, pressure, sample doping, substrates, etc.). Even a small change in any of these factors can induce switching of the ground state. In such a situation, when a wide class of the materials exhibit multiple transitions under weak variation of the parameters, a convenient classification scheme of the possible ground states is of significant help.

This paper is dedicated to theoretical study of an electronic liquid of AA bilayer graphene (AA-BLG), a topic that attracted attention in recent years [12–20]. A specific question we would like to address here is the problem of classifying low-temperature nonsuperconducting ordered states of AA-BLG. The investigation of this relatively simple system can help us to extend the proposed approach to other types of orders (superconducting, in particular) and other types of systems, such as twisted and AB-BLG.

The present discussion is built on the approach previously used in Ref. [21] to study multiple possible order parameters in the AB-BLG. Adopting that technique for the AA-BLG electronic liquid, we will formulate an approximate Hamiltonian that possesses an SU(4) symmetry in the spin-valley index space at zero doping. Following Ref. [21], we assume that the main interaction in the system is a long-range Coulomb electron-electron coupling and neglect any additional interactions (e.g., electron-lattice). Mean field (matrix) self-consistency equation for such an AA-BLG model reveals several competing nonsuperconducting ordered states characterized by a matrix order parameter.

Studying the self-consistency equation, one finds that its solutions could be both Hermitian and non-Hermitian matrices. The former case was considered in Ref. [21]. It has been shown that the signature of the order-parameter matrix can be used for exhaustive classification of the ordered states. Here we analyze also the non-Hermitian solutions to the self-consistency equation. These solutions are characterized by finite interlayer currents that can carry, not only electric charge, but also spin-related and/or valley-related quanta, depending on the specific details. A broad array of the ordered states compatible with our self-consistency equation suggests that the true ground state of the AA-BLG may depend on variety of details, some of which could be purposefully tailored to stabilize a desired order parameter.

The paper is organized as follows. In Sec. II we formulate an SU(4)-symmetric model of the AA-BLG. In Sec. III we derive the self-consistency mean field equation for the multicomponent order parameter described by 4×4 matrix $\hat{Q}$. In Sec. IV we describe the solutions of this mean field equations. Three different cases are considered: Hermitian $\hat{Q}$, anti-Hermitian $\hat{Q}$, and matrix $\hat{Q}$ that is neither Hermitian nor anti-Hermitian (non-Hermitian and non-anti-Hermitian $\hat{Q}$). Section V is devoted to discussion. Some details of derivation of the mean field equation are placed in the Appendix.

II. MODEL

A. Tight-binding kinetic energy for AA-BLG

A sample of the AA-BLG consists of two graphene layers and every carbon atom of the top layer is directly above one of the carbon atoms in the bottom layer. Single-electron hopping Hamiltonian for the AA-BLG can be written as [15]

$$\hat{H}_0 = -t \sum_{\langle \mathbf{mn}\rangle l\sigma} (\hat{d}^\dagger_{\mathbf{m}lA\sigma}\hat{d}_{\mathbf{n}lB\sigma} + \text{H.c.}) - t_0 \sum_{\mathbf{n}a\sigma} (\hat{d}^\dagger_{\mathbf{n}1a\sigma}\hat{d}_{\mathbf{n}2a\sigma} + \text{H.c.}). \quad (1)$$

Here $\hat{d}^\dagger_{\mathbf{n}la\sigma}$ and $\hat{d}_{\mathbf{n}la\sigma}$ are the creation and annihilation operators of an electron with spin projection σ in the layer $l = 1, 2$ on the sublattice $a = A, B$ at the unit cell $\mathbf{n}$; and $\langle \dots \rangle$ denotes a nearest-neighbor pair. The amplitude $t = 2.7$ eV ($t_0 = 0.35$ eV) in Eq. (1) describes the in-plane (interplane) nearest-neighbor hopping.

To diagonalize the hopping Hamiltonian it is convenient to switch to momentum representation. For a sample with N_c unit cells in a single graphene layer this is achieved by the Fourier transformation

$$\hat{d}_{\mathbf{k}la\sigma} = \frac{e^{-ia\varphi_{\mathbf{k}}}}{\sqrt{N_c}} \sum_{\mathbf{n}} e^{i\mathbf{k}\cdot\mathbf{n}} \hat{d}_{\mathbf{n}la\sigma}. \quad (2)$$

Here the numerical values of the sublattice index a are $a = 0$ for sublattice A, and $a = 1$ for sublattice B. The phase factor in Eq. (2) is $\exp(i\varphi_{\mathbf{k}}) = f_{\mathbf{k}}/|f_{\mathbf{k}}|$, the function $f_{\mathbf{k}}$ being

$$f_{\mathbf{k}} = 1 + 2\exp\left(\frac{3ik_x a_0}{2}\right)\cos\left(\frac{\sqrt{3}k_y a_0}{2}\right), \quad (3)$$

and a_0 is the in-plane carbon-carbon distance. Quasimomentum vectors are confined to the graphene Brillouin zone, which has a shape of a regular hexagon with two independent Dirac points in two corners [22]:

$$\mathbf{K}_{1,2} = \frac{2\pi}{3\sqrt{3}a_0}(\sqrt{3}, \pm 1). \quad (4)$$

Four more corners of the Brillouin zone can be found by two 60° rotations of $\mathbf{K}_{1,2}$ (see Fig. 1).

In the momentum representation, the hopping Hamiltonian becomes

$$\hat{H}_0 = \sum_{\mathbf{k}\sigma} \hat{\Psi}^\dagger_{\mathbf{k}\sigma} \hat{\mathcal{H}}_{\mathbf{k}} \hat{\Psi}_{\mathbf{k}\sigma}, \quad (5)$$

where the matrix $\hat{\mathcal{H}}_{\mathbf{k}}$ and the bispinor $\hat{\Psi}^\dagger_{\mathbf{k}\sigma}$ are

$$\hat{\mathcal{H}}_{\mathbf{k}} = -\begin{pmatrix} 0 & t_0 & t|f_{\mathbf{k}}| & 0 \\ t_0 & 0 & 0 & t|f_{\mathbf{k}}| \\ t|f_{\mathbf{k}}| & 0 & 0 & t_0 \\ 0 & t|f_{\mathbf{k}}| & t_0 & 0 \end{pmatrix}, \quad (6)$$

$$\hat{\Psi}^\dagger_{\mathbf{k}\sigma} = (\hat{d}^\dagger_{\mathbf{k}1A\sigma}, \hat{d}^\dagger_{\mathbf{k}2A\sigma}, \hat{d}^\dagger_{\mathbf{k}1B\sigma}, \hat{d}^\dagger_{\mathbf{k}2B\sigma}). \quad (7)$$

Thus, the Hamiltonian (1) can be diagonalized as

$$\hat{H}_0 = \sum_{\mathbf{k}s\sigma} \epsilon^{(s)}_{\mathbf{k}} \hat{\gamma}^\dagger_{\mathbf{k}s\sigma} \hat{\gamma}_{\mathbf{k}s\sigma}, \quad (8)$$

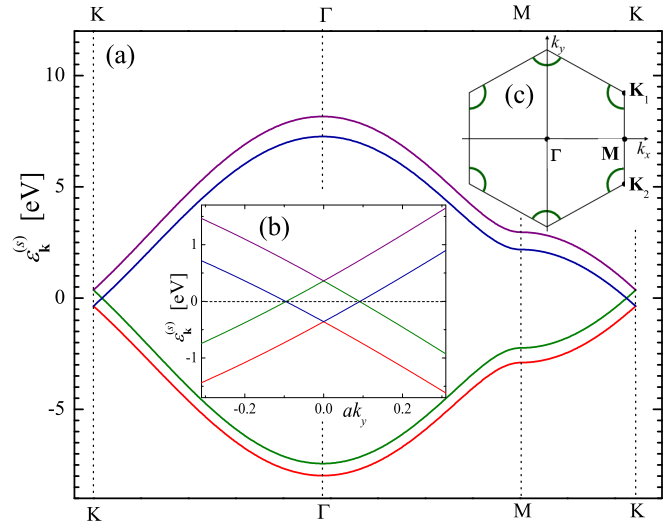

FIG. 1. (a) The single-particle band structure of the AA-BLG. The spectrum consists of four bands $\epsilon^{(s)}_{\mathbf{k}}$ [see Eqs. (9) and (10)]. (b) The spectrum near the Dirac points can be approximately linearized [see Eqs. (22) and (23)]. The intersection of the bands $s = 2$ and 3 occurs exactly at zero energy, which corresponds to the Fermi level of the undoped system. (c) The first Brillouin zone (hexagon) of the AA-BLG. The circles around the Dirac points correspond to Fermi surfaces.

where the band eigenenergies $\epsilon^{(s)}_{\mathbf{k}}$ are

$$\epsilon^{(1)}_{\mathbf{k}} = -t_0 - t|f_{\mathbf{k}}|, \quad \epsilon^{(2)}_{\mathbf{k}} = -t_0 + t|f_{\mathbf{k}}|, \quad (9)$$

$$\epsilon^{(3)}_{\mathbf{k}} = +t_0 - t|f_{\mathbf{k}}|, \quad \epsilon^{(4)}_{\mathbf{k}} = +t_0 + t|f_{\mathbf{k}}|. \quad (10)$$

This energy spectrum is plotted in Fig. 1(a).

The band operators $\hat{\gamma}_{\mathbf{k}s\sigma}$ are connected to $\hat{d}_{\mathbf{k}la\sigma}$ as follows:

$$\hat{d}_{\mathbf{k}la\sigma} = \tfrac{1}{2}[\hat{\gamma}_{\mathbf{k}1\sigma} + (-1)^a\hat{\gamma}_{\mathbf{k}2\sigma} + (-1)^l\hat{\gamma}_{\mathbf{k}3\sigma} + (-1)^{a+l}\hat{\gamma}_{\mathbf{k}4\sigma}], \quad (11)$$

where $l = 0$ for layer 1 and $l = 1$ for layer 2. The latter relation is easy to invert and we find that

$$\hat{\gamma}_{\mathbf{k}1\sigma} = \frac{1}{2}\sum_{la}\hat{d}_{\mathbf{k}la\sigma}, \quad \hat{\gamma}_{\mathbf{k}2\sigma} = \frac{1}{2}\sum_{la}(-1)^a\hat{d}_{\mathbf{k}la\sigma}, \quad (12)$$

$$\hat{\gamma}_{\mathbf{k}3\sigma} = \frac{1}{2}\sum_{la}(-1)^l\hat{d}_{\mathbf{k}la\sigma}, \quad \hat{\gamma}_{\mathbf{k}4\sigma} = \frac{1}{2}\sum_{la}(-1)^{l+a}\hat{d}_{\mathbf{k}la\sigma}. \quad (13)$$

Analyzing spectra (9) and (10) one notices that the bands $s = 2, 3$ cross the Fermi level $\varepsilon = 0$. The corresponding Fermi surfaces can be approximated by circles of radius $k_F = 2t_0/(3ta_0)$ centered around the Brillouin zone corners (the Dirac points), as shown in Fig. 1(c). At the same time, the bands $s = 1, 4$ do not reach the Fermi level, and have no Fermi surface.

B. Valley quantum number

For graphene-based systems it is often useful to introduce a binary-valued valley index $\xi = 1, 2$: an electronic state with the quasimomentum $\mathbf{k}$ is assumed to be in valley $\mathbf{K}_\xi$ if

$|\mathbf{k}-\mathbf{K}_\xi| < q_0$, where the valley radius $q_0 = |\mathbf{K}_1 - \mathbf{K}_2|/2$ equals $q_0 = 2\pi/3\sqrt{3}a_0$. The states whose momenta lie outside either valley $\mathbf{K}_1$ or valley $\mathbf{K}_2$ are high-energy states. Such states will be discarded since their contribution to the low-energy physics is insignificant. Further, we will count the quasimomentum $\mathbf{k}$ relative to the valley centers $\mathbf{K}_{1,2}$. We expand the function $f_{\mathbf{K}_\xi+\mathbf{k}}$ near each Dirac point and in the linear approximation obtain

$$f_{\mathbf{K}_\xi+\mathbf{k}} = \frac{3a_0}{2}[k_y + (-1)^\xi i k_x]. \tag{14}$$

Since we are interested here only in the low-energy states, we will use linear approximation (14) within the valleys.

We define new single-electron operators in a specific valley as

$$\hat{\gamma}_{\mathbf{k}s\xi\sigma} = \begin{cases} \hat{\gamma}_{\mathbf{K}_1+\mathbf{k}s\sigma}, & \text{if } \xi = 1 \\ (-1)^{s+1} e^{i\phi_\mathbf{k}} \hat{\gamma}_{\mathbf{K}_2+\mathbf{k}s\sigma}, & \text{if } \xi = 2 \end{cases} \tag{15}$$

where the phase factor $\exp(i\phi_\mathbf{k})$ is equal to

$$e^{i\phi_\mathbf{k}} = -\frac{ik_x + k_y}{|\mathbf{k}|}. \tag{16}$$

As it follows from Eq. (14), it is connected with the complex phases near the valley centers $\mathbf{K}_{1,2}$:

$$e^{i\varphi_{\mathbf{K}_1+\mathbf{k}}} = -e^{-i\phi_\mathbf{k}}, \quad e^{i\varphi_{\mathbf{K}_2+\mathbf{k}}} = e^{i\phi_\mathbf{k}}. \tag{17}$$

Using Eqs. (11) and (15), one can write $\hat{d}_{\mathbf{n}la\sigma}$ in terms of $\hat{\gamma}_{\mathbf{k}s\xi\sigma}$. To this purpose, it is convenient to introduce the valley-specific operator $\hat{d}_{\mathbf{k}la\xi\sigma} = \hat{d}_{\mathbf{K}_\xi+\mathbf{k}la\sigma}$, and write

$$\hat{d}_{\mathbf{k}la\xi\sigma} = \begin{cases} \hat{\mathfrak{g}}_{\mathbf{k}la\xi\sigma}, & \text{if } \xi = 1 \\ e^{-i\phi_\mathbf{k}} \hat{\mathfrak{g}}_{\mathbf{k}l\bar{a}\xi\sigma}, & \text{if } \xi = 2. \end{cases} \tag{18}$$

In this definition, the operators $\hat{\mathfrak{g}}_{\mathbf{k}la\xi\sigma}$ are linear combinations of the band operators

$$\begin{aligned}\hat{\mathfrak{g}}_{\mathbf{k}la\xi\sigma} = \tfrac{1}{2}[&\hat{\gamma}_{\mathbf{k}1\xi\sigma} + (-1)^a \hat{\gamma}_{\mathbf{k}2\xi\sigma} + (-1)^l \hat{\gamma}_{\mathbf{k}3\xi\sigma} \\ &+ (-1)^{a+l} \hat{\gamma}_{\mathbf{k}4\xi\sigma}],\end{aligned} \tag{19}$$

and we adhere to the convention that a bar over a binary-valued index inverts its value (i.e., if $a = A$, then $\bar{a} = B$, and vice versa).

There is an obvious disparity between the valleys in definitions (15) and (18). Note that the sublattice index in Eq. (18) is inverted for $\xi = 2$. In addition, the phase factors in (15) are not identical in different valleys. The same is true for Eq. (18). We will see below that such a phase factor choice is needed to make explicit the SU(4) symmetry of the interaction term.

Inverting relation (2) and using the valley-specific operators in $\mathbf{k}$ space, we can approximate the real-space operators as follows:

$$\begin{aligned}\hat{d}_{\mathbf{n}la\sigma} \approx \frac{1}{\sqrt{N_c}} \sum_{|\mathbf{k}|<q_0} [&e^{-ia\phi_\mathbf{k} - i\mathbf{K}_1\cdot\mathbf{n}} (-1)^a \hat{\mathfrak{g}}_{\mathbf{k}la\mathbf{K}_1\sigma} \\ &+ e^{-i\bar{a}\phi_\mathbf{k} - i\mathbf{K}_2\cdot\mathbf{n}} \hat{\mathfrak{g}}_{\mathbf{k}l\bar{a}\mathbf{K}_2\sigma}] e^{-i\mathbf{k}\cdot\mathbf{n}}.\end{aligned} \tag{20}$$

This expression disregards all high-energy states that lie outside the valleys.

C. SU(4)-symmetric single-electron Hamiltonian

Within the developed formalism the Hamiltonian (8) can be approximated as

$$\hat{H}_0 \approx \sum_{s,|\mathbf{k}|<q_0} \varepsilon_\mathbf{k}^{(s)} \sum_{\xi\sigma} \hat{\gamma}^\dagger_{\mathbf{k}s\xi\sigma} \hat{\gamma}_{\mathbf{k}s\xi\sigma}, \tag{21}$$

where $\varepsilon_\mathbf{k}^{(s)}$ are linear approximations to the exact eigenenergies $\epsilon_\mathbf{k}^{(s)}$ near the Dirac points

$$\varepsilon_\mathbf{k}^{(1)} = -t_0 - v_\mathrm{F}|\mathbf{k}|, \quad \varepsilon_\mathbf{k}^{(2)} = -t_0 + v_\mathrm{F}|\mathbf{k}|, \tag{22}$$

$$\varepsilon_\mathbf{k}^{(3)} = +t_0 - v_\mathrm{F}|\mathbf{k}|, \quad \varepsilon_\mathbf{k}^{(4)} = +t_0 + v_\mathrm{F}|\mathbf{k}|. \tag{23}$$

The Fermi velocity in these expressions is equal to $v_\mathrm{F} = 3a_0 t/2$ ($\hbar = 1$).

The significance of formula (21) is that it explicitly demonstrates the valley degeneracy of the single-electron spectrum of AA-BLG, and, additionally, it reveals the SU(4) symmetry of the model. To illustrate this important point we introduce the spin-valley muti-index $m = (\xi, \sigma)$, which takes four possible values. This allows us to abbreviate the notation as follows $\hat{\gamma}_{\mathbf{k}s\xi\sigma} = \hat{\gamma}_{\mathbf{k}sm}$. Any 4×4 unitary matrix $\hat{U} \in$ SU(4), with matrix elements $u_{mm'}$, defines a Bogolyubov transform

$$\hat{\gamma}_{\mathbf{k}sm} \to \sum_{m'} u_{mm'} \hat{\gamma}_{\mathbf{k}sm'}. \tag{24}$$

It is easy to check that this transformation leaves Hamiltonian (21) unchanged.

D. Interaction term

The most general form of the interaction term for AA-BLG is

$$\hat{H}_\mathrm{int} = \frac{1}{2N_c} \sum_{\mathbf{k}ll'aa'} V^{ll'}_{\mathbf{k}aa'} \hat{\rho}_{\mathbf{k}la} \hat{\rho}_{-\mathbf{k}l'a'}. \tag{25}$$

Vector $\mathbf{k}$ here is the transferred momentum, parameters $V^{ll'}_{\mathbf{k}aa'}$ are the Fourier components of the potential energy $V^{ll'}_{aa'}(\mathbf{R})$ describing the interaction between an electron in layer l, sublattice a and another electron in layer l', sublattice a'. Finally, $\hat{\rho}_{\mathbf{k}la}$ is the Fourier component of a single-site particle-density operator $\hat{\rho}_{\mathbf{n}la} = \sum_\sigma \hat{d}^\dagger_{\mathbf{n}la\sigma} \hat{d}_{\mathbf{n}la\sigma}$.

For small transferred momentum $\mathbf{k}$ one has $\hat{\rho}_{\mathbf{k}la} = \hat{\rho}^{\mathbf{K}_1}_{\mathbf{k}la} + \hat{\rho}^{\mathbf{K}_2}_{\mathbf{k}la}$, where two chiral density components can be expressed as

$$\hat{\rho}^{\xi}_{\mathbf{k}la} = \sum_{\mathbf{q}\sigma} e^{ia(\varphi_{\mathbf{K}_\xi+\mathbf{k}+\mathbf{q}} - \varphi_{\mathbf{K}_\xi+\mathbf{q}})} \hat{d}^\dagger_{\mathbf{q}la\xi\sigma} \hat{d}_{\mathbf{k}+\mathbf{q}la\xi\sigma} \tag{26}$$

or, equivalently, in terms of the band operators as

$$\hat{\rho}^{\mathbf{K}_1}_{\mathbf{k}la} = \sum_{\mathbf{q}\sigma} e^{-ia(\phi_{\mathbf{k}+\mathbf{q}} - \phi_\mathbf{q})} \hat{\mathfrak{g}}^\dagger_{\mathbf{q}la\mathbf{K}_1\sigma} \hat{\mathfrak{g}}_{\mathbf{k}+\mathbf{q}la\mathbf{K}_1\sigma}, \tag{27}$$

$$\hat{\rho}^{\mathbf{K}_2}_{\mathbf{k}la} = \sum_{\mathbf{q}\sigma} e^{-i\bar{a}(\phi_{\mathbf{k}+\mathbf{q}} - \phi_\mathbf{q})} \hat{\mathfrak{g}}^\dagger_{\mathbf{q}l\bar{a}\mathbf{K}_2\sigma} \hat{\mathfrak{g}}_{\mathbf{k}+\mathbf{q}l\bar{a}\mathbf{K}_2\sigma}. \tag{28}$$

Both $\hat{\rho}^{\xi}_{\mathbf{k}la}$ vary smoothly in space for small $\mathbf{k}$. Aside from $\hat{\rho}^{\xi}_{\mathbf{k}la}$, there is an oscillating contribution to the density

$$\hat{\rho}^{\xi\bar{\xi}}_{\mathbf{k}la} = \sum_{\mathbf{q}\sigma} e^{ia(\varphi_{\mathbf{K}_\xi+\mathbf{k}+\mathbf{q}} - \varphi_{\mathbf{K}_\xi+\mathbf{q}})} \hat{d}^\dagger_{\mathbf{q}la\xi\sigma} \hat{d}_{\mathbf{k}+\mathbf{q}la\xi\sigma}. \tag{29}$$

The wave vector corresponding to the spatial modulation of $\hat{\rho}^{\xi\bar{\xi}}_{\mathbf{k}la}$ is never small: it is of order of $\mathbf{K}_1 - \mathbf{K}_2$ even for small $\mathbf{k}$.

Since the density operator has smooth as well as oscillating contributions, the interaction can be split into the forward scattering $\hat{H}_\mathrm{f}$ and back scattering $\hat{H}_\mathrm{b}$:

$$\hat{H}_\mathrm{int} = \hat{H}_\mathrm{f} + \hat{H}_\mathrm{b}, \tag{30}$$

$$\hat{H}_\mathrm{f} = \frac{1}{2N_c} \sum_{\substack{\mathbf{k}\xi\xi' \\ ll'aa'}} V^{ll'}_{\mathbf{k}aa'} \hat{\rho}^{\xi}_{\mathbf{k}la} \hat{\rho}^{\xi'}_{-\mathbf{k}l'a'}, \tag{31}$$

$$\hat{H}_\mathrm{b} = \frac{1}{2N_c} \sum_{\mathbf{k}\xi ll'aa'} V^{ll'}_{\mathbf{K}_1-\mathbf{K}_2aa'} \hat{\rho}^{\xi\bar{\xi}}_{\mathbf{k}la} \hat{\rho}^{\bar{\xi}\xi}_{-\mathbf{k}l'a'}. \tag{32}$$

As one can see, $\hat{H}_\mathrm{f}$ describes scattering in which both participating electrons maintain their valley indices after scattering, while $\hat{H}_\mathrm{b}$ represents large-momentum scattering, when participating electrons from different valleys exchange their valley indices.

We assume here that the electron-electron interaction is sufficiently long range. In this case $V^{ll'}_{\mathbf{K}_1-\mathbf{K}_2aa'} < V^{ll'}_{\mathbf{k}aa'}$ since $|\mathbf{k}| < |\mathbf{K}_1 - \mathbf{K}_2|$. For this reason we neglect below the back scattering (this issue will be discussed in Sec. V in more detail). Since the considered interaction is a long-range one, we can assume that the coupling is approximately independent of the sublattice indices:

$$V^{ll'}_{\mathbf{k}aa'} \approx V^{ll'}_{\mathbf{k}}. \tag{33}$$

Under these approximations, the interaction (25) reads as

$$\hat{H}_\mathrm{int} = \frac{1}{2N_c} \sum_{\mathbf{k}ll'} V^{ll'}_{\mathbf{k}} \hat{\rho}_{\mathbf{k}l} \hat{\rho}_{-\mathbf{k}l'}, \tag{34}$$

where the smooth density component in layer l is

$$\hat{\rho}_{\mathbf{k}l} = \sum_{a\xi} \hat{\rho}^{\xi}_{\mathbf{k}la} = \sum_{\mathbf{q}am} e^{ia(\phi_\mathbf{q} - \phi_{\mathbf{k}+\mathbf{q}})} \hat{\mathfrak{g}}^\dagger_{\mathbf{q}lam} \hat{\mathfrak{g}}_{\mathbf{k}+\mathbf{q}lam}. \tag{35}$$

In the latter formula we used the multi-index notation $m = (\xi, \sigma)$. This serves a twofold purpose. For one, it makes the expression more concise. Additionally, it explicitly reveals the invariance of $\hat{\rho}_{\mathbf{k}l}$ under the action of the SU(4) Bogolyubov transformation (24). At this point one can appreciate the motivation behind the complexity of formulas (15) and (18). If multiple phase factors were not absorbed in the definitions of the valley-specific operators, these phase factors would emerge in Eq. (35), obscuring the invariance. Finally, we observe that, since the operator $\hat{\rho}_{\mathbf{k}l}$ possesses the SU(4) invariance, the same is true for the interaction (34).

E. Effective model

As it was stated above, only two of the four single-electron bands form the Fermi surface at zero doping (see Fig. 1). Therefore, the high-energy bands $s = 1, 4$ can not modify significantly the low-energy physics of the AA-BLG. We discarded these bands from the model, which simplifies considerably further analysis. In this approximation the single-electron Hamiltonian becomes

$$\hat{H}^\mathrm{eff}_0 = \sum_{\mathbf{k}\xi\sigma} (v_\mathrm{F}|\mathbf{k}| - t_0)(\hat{\gamma}^\dagger_{\mathbf{k}2\xi\sigma} \hat{\gamma}_{\mathbf{k}2\xi\sigma} - \hat{\gamma}^\dagger_{\mathbf{k}3\xi\sigma} \hat{\gamma}_{\mathbf{k}3\xi\sigma}). \tag{36}$$

The density operator $\hat{\rho}_{\mathbf{k}l}$ reduces to

$$\hat{\rho}_{\mathbf{k}l} \approx \frac{1}{4} \sum_{\mathbf{q}am} e^{ia(\phi_\mathbf{q} - \phi_{\mathbf{q}+\mathbf{k}})} [\hat{\gamma}^\dagger_{\mathbf{q}2m} + (-1)^{l+a} \hat{\gamma}^\dagger_{\mathbf{q}3m}] \times [\hat{\gamma}_{\mathbf{q}+\mathbf{k}2m} + (-1)^{l+a} \hat{\gamma}_{\mathbf{q}+\mathbf{k}3m}]. \tag{37}$$

Substituting this expression in Eq. (34) one derives

$$\hat{H}^\mathrm{eff}_\mathrm{int} = \hat{H}^\mathrm{eff}_\mathrm{dir} + \hat{H}^\mathrm{eff}_\mathrm{ex} + \hat{H}^\mathrm{eff}_\mathrm{u}, \tag{38}$$

where the direct term is defined as

$$\hat{H}^\mathrm{eff}_\mathrm{dir} = \frac{1}{16N_c} \sum_{\mathbf{q}\mathbf{q}'\mathbf{k}mm'} V_+(\mathbf{k})[1 + e^{i(\phi_\mathbf{q} - \phi_{\mathbf{q}+\mathbf{k}})}] \times [1 + e^{i(\phi_{\mathbf{q}'} - \phi_{\mathbf{q}'-\mathbf{k}})}](\hat{\gamma}^\dagger_{\mathbf{q}2m} \hat{\gamma}_{\mathbf{q}+\mathbf{k}2m} + \hat{\gamma}^\dagger_{\mathbf{q}3m} \hat{\gamma}_{\mathbf{q}+\mathbf{k}3m}) \times (\hat{\gamma}^\dagger_{\mathbf{q}'2m'} \hat{\gamma}_{\mathbf{q}'-\mathbf{k}2m'} + \hat{\gamma}^\dagger_{\mathbf{q}'3m'} \hat{\gamma}_{\mathbf{q}'-\mathbf{k}3m'}), \tag{39}$$

the exchange term is

$$\hat{H}^\mathrm{eff}_\mathrm{ex} = \frac{1}{16N_c} \sum_{\mathbf{q}\mathbf{q}'\mathbf{k}mm'} V_-(\mathbf{k})[1 - e^{i(\phi_\mathbf{q} - \phi_{\mathbf{q}+\mathbf{k}})}] \times [1 - e^{i(\phi_{\mathbf{q}'} - \phi_{\mathbf{q}'-\mathbf{k}})}](\hat{\gamma}^\dagger_{\mathbf{q}2m} \hat{\gamma}_{\mathbf{q}+\mathbf{k}3m} \hat{\gamma}^\dagger_{\mathbf{q}'3m'} \hat{\gamma}_{\mathbf{q}'-\mathbf{k}2m'} + \hat{\gamma}^\dagger_{\mathbf{q}3m} \hat{\gamma}_{\mathbf{q}+\mathbf{k}2m} \hat{\gamma}^\dagger_{\mathbf{q}'2m'} \hat{\gamma}_{\mathbf{q}'-\mathbf{k}3m'}), \tag{40}$$

and the umklapp term is

$$\hat{H}^\mathrm{eff}_\mathrm{u} = \frac{1}{16N_c} \sum_{\mathbf{q}\mathbf{q}'\mathbf{k}mm'} V_-(\mathbf{k})[1 - e^{i(\phi_\mathbf{q} - \phi_{\mathbf{q}+\mathbf{k}})}] \times [1 - e^{i(\phi_{\mathbf{q}'} - \phi_{\mathbf{q}'-\mathbf{k}})}](\hat{\gamma}^\dagger_{\mathbf{q}2m} \hat{\gamma}_{\mathbf{q}+\mathbf{k}3m} \hat{\gamma}^\dagger_{\mathbf{q}'2m'} \hat{\gamma}_{\mathbf{q}'-\mathbf{k}3m'} + \hat{\gamma}^\dagger_{\mathbf{q}3m} \hat{\gamma}_{\mathbf{q}+\mathbf{k}2m} \hat{\gamma}^\dagger_{\mathbf{q}'3m'} \hat{\gamma}_{\mathbf{q}'-\mathbf{k}2m'}). \tag{41}$$

In these approximate expressions we introduced layer-symmetric and layer-antisymmetric interactions $V_\pm(\mathbf{k}) = (V^{11}_\mathbf{k} \pm V^{12}_\mathbf{k})$. We also used the relation $\sum_{ll'} (-1)^l V^{ll'}_\mathbf{k} \equiv 0$, which can be trivially checked.

F. Symmetry group of the effective model

Observe that the operators $\hat{H}^\mathrm{eff}_0$, $\hat{H}^\mathrm{eff}_\mathrm{dir}$, $\hat{H}^\mathrm{eff}_\mathrm{ex}$, and $\hat{H}^\mathrm{eff}_\mathrm{u}$, which constitute the effective model Hamiltonian, are individually SU(4) invariant. Indeed, each of these operators are explicitly composed of the bilinears $\mathcal{I}^{sr}_\mathbf{qp}$ defined as

$$\mathcal{I}^{sr}_\mathbf{qp} = \sum_m \hat{\gamma}^\dagger_{\mathbf{q}sm} \hat{\gamma}_{\mathbf{p}rm}, \quad s, r = 2, 3 \tag{42}$$

that are invariants of the SU(4) Bogolyubov transformation (24). Besides, the effective Hamiltonian evidently remains unchanged upon the substitution

$$\hat{\gamma}_{\mathbf{p}sm} \to (-1)^s \hat{\gamma}_{\mathbf{p}sm}. \tag{43}$$

This allows us to change the relative sign between $\hat{\gamma}_{\mathbf{p}3m}$ and $\hat{\gamma}_{\mathbf{p}2m}$, without changing the Hamiltonian.

From the standpoint of the AA-BLG lattice structure, the substitution (43) corresponds to either switching the layers

$$(\text{top layer}) \leftrightarrow (\text{bottom layer}), \tag{44}$$

or switching the sublattices

$$(\text{sublattice } A) \leftrightarrow (\text{sublattice } B), \tag{45}$$

as it follows from relation (11). Consequently, the symmetry (43) can be viewed as a manifestation of the layer equivalence, or manifestation of the sublattice equivalence (at the level of our effective model these two equivalences cannot be distinguished).

Transformation (43), together with the identity transformation, constitutes the $\mathbb{Z}_2$ group. Since the transformations (24) and (43) commute with each other, we conclude that the symmetry group of the effective Hamiltonian is

$$G \cong \mathrm{SU}(4) \times \mathbb{Z}_2. \tag{46}$$

However, the symmetry group of $\hat{H}_0^{\mathrm{eff}}$ and $\hat{H}_{\mathrm{dir}}^{\mathrm{eff}}$ is broader than G: one can check directly that both $\hat{H}_0^{\mathrm{eff}}$ and $\hat{H}_{\mathrm{dir}}^{\mathrm{eff}}$ are composed of the bilinears $\mathcal{I}_{\mathbf{qp}}^{sr}$ with identical band indices $s = r$. Thus, $\hat{H}_0^{\mathrm{eff}}$ and $\hat{H}_{\mathrm{dir}}^{\mathrm{eff}}$ remain invariant even when a Bogolyubov rotation for $s = 2$ band is nonidentical to the rotation for $s = 3$ band. In other words, when $V_- \equiv 0$, the model's symmetry group expands to

$$G_0 \cong \mathrm{SU}(4) \times \mathrm{SU}(4). \tag{47}$$

We will see below that the broader symmetry group corresponds to broader set of solutions for a self-consistency equation.

III. MEAN FIELD APPROXIMATION

We apply the mean field approach to the effective Hamiltonian

$$\hat{H}^{\mathrm{eff}} = \hat{H}_0^{\mathrm{eff}} + \hat{H}_{\mathrm{int}}^{\mathrm{eff}} \tag{48}$$

with the aim of exploring (nonsuperconducting) symmetry-breaking ordered phases of our model. Implementing the mean field decoupling for $\hat{H}_{\mathrm{dir}}^{\mathrm{eff}}$, we obtain

$$\hat{H}_{\mathrm{dir}}^{\mathrm{MF}} = -\frac{1}{8N_c}\sum_{\substack{\mathbf{qp}\\ mm'}} V_+(\mathbf{p}-\mathbf{q})\left|1+e^{i(\phi_{\mathbf{q}}-\phi_{\mathbf{p}})}\right|^2 \times (\langle\hat{\gamma}^\dagger_{\mathbf{p}3m'}\hat{\gamma}_{\mathbf{p}2m}\rangle\hat{\gamma}^\dagger_{\mathbf{q}2m}\hat{\gamma}_{\mathbf{q}3m'} + \hat{\gamma}^\dagger_{\mathbf{p}3m'}\hat{\gamma}_{\mathbf{p}2m}\langle\hat{\gamma}^\dagger_{\mathbf{q}2m}\hat{\gamma}_{\mathbf{q}3m'}\rangle), \tag{49}$$

where $\langle\dots\rangle$ stands for the ground-state average.

It is convenient to introduce the 4×4 operator-valued matrix $\hat{\Theta}_{\mathbf{q}}$ whose elements are

$$\Theta_{\mathbf{q}mm'} = \hat{\gamma}^\dagger_{\mathbf{q}3m}\hat{\gamma}_{\mathbf{q}2m'}. \tag{50}$$

Assuming that the average $\langle\hat{\Theta}_{\mathbf{q}}\rangle$ depends only on the absolute value of the vector $\mathbf{q}$, we write the following compact expression:

$$\hat{H}_{\mathrm{dir}}^{\mathrm{MF}} = -\frac{1}{N_c}\sum_{\mathbf{qp}}\bar{V}_+\mathrm{Tr}(\langle\hat{\Theta}_{\mathbf{p}}\rangle\hat{\Theta}^\dagger_{\mathbf{q}} + \langle\hat{\Theta}^\dagger_{\mathbf{p}}\rangle\hat{\Theta}_{\mathbf{q}}). \tag{51}$$

Deriving this formula we replace the interaction function $V_+(\mathbf{p}-\mathbf{q})$ by its average value at the Fermi surface. The constant $\bar{V}_+$ is equal to

$$\bar{V}_+ = \frac{1}{4}\int_0^{2\pi}\frac{d\chi}{2\pi}(1+\cos\chi)V_+(k_{\mathrm{F}}\sqrt{2-2\cos\chi}). \tag{52}$$

Likewise, the mean field form of the umklapp interaction is

$$\hat{H}_{\mathrm{u}}^{\mathrm{MF}} = -\frac{1}{N_c}\sum_{\mathbf{qp}}\bar{V}_-\mathrm{Tr}\,(\langle\hat{\Theta}_{\mathbf{p}}\rangle\hat{\Theta}_{\mathbf{q}} + \langle\hat{\Theta}^\dagger_{\mathbf{p}}\rangle\hat{\Theta}^\dagger_{\mathbf{q}}), \tag{53}$$

$$\bar{V}_- = \frac{1}{4}\int_0^{2\pi}\frac{d\chi}{2\pi}(1-\cos\chi)V_-(k_{\mathrm{F}}\sqrt{2-2\cos\chi}). \tag{54}$$

As for $\hat{H}_{\mathrm{ex}}$, it does not contribute to the mean field Hamiltonian. Indeed, one can check that nonzero expectation value $\langle\hat{\gamma}^\dagger_{\mathbf{q}3m}\hat{\gamma}_{\mathbf{q}2m'}\rangle$ in Eq. (40) is possible only at zero transferred momentum $\mathbf{k} = 0$. Contributions with vanishing transferred momentum in $\hat{H}_{\mathrm{ex}}^{\mathrm{eff}}$ vanish due to

$$1 - e^{i(\phi_{\mathbf{q}}-\phi_{\mathbf{q}+\mathbf{k}})} = 1 - e^{i(\phi_{\mathbf{q}'}-\phi_{\mathbf{q}'-\mathbf{k}})} = 0 \tag{55}$$

at $\mathbf{k} = 0$.

The resultant mean field Hamiltonian reads as

$$\hat{H}^{\mathrm{MF}} = \hat{H}_0^{\mathrm{eff}} + \hat{H}_{\mathrm{int}}^{\mathrm{MF}}, \tag{56}$$

where the mean field interaction is

$$\hat{H}_{\mathrm{int}}^{\mathrm{MF}} = -\sum_{\mathbf{q}}\mathrm{Tr}(\hat{Q}^\dagger\hat{\Theta}_{\mathbf{q}} + \hat{\Theta}^\dagger_{\mathbf{q}}\hat{Q}). \tag{57}$$

In this expression the 4×4 matrix $\hat{Q}$ is the order parameter

$$\hat{Q} = \frac{1}{N_c}\sum_{\mathbf{p}}(\bar{V}_+\langle\hat{\Theta}_{\mathbf{p}}\rangle + \bar{V}_-\langle\hat{\Theta}^\dagger_{\mathbf{p}}\rangle). \tag{58}$$

To derive a self-consistency equation, it is convenient to invert this definition

$$\frac{1}{N_c}\sum_{\mathbf{p}}\langle\hat{\Theta}_{\mathbf{p}}\rangle = \frac{1}{\bar{V}_+^2-\bar{V}_-^2}(\bar{V}_+\hat{Q} - \bar{V}_-\hat{Q}^\dagger). \tag{59}$$

We prove in the Appendix that for our mean field Hamiltonian $\hat{H}^{\mathrm{MF}}$ the symmetry-breaking average $\langle\hat{\Theta}_{\mathbf{p}}\rangle$ satisfies

$$\frac{1}{N_c}\sum_{\mathbf{p}}\langle\hat{\Theta}_{\mathbf{p}}\rangle = \frac{1}{2N_c}\sum_{\mathbf{k}}\hat{Q}\left(\varepsilon_{\mathbf{k}}^2 + \hat{Q}^\dagger\hat{Q}\right)^{-\frac{1}{2}}. \tag{60}$$

We consider only the undoped system, where the Fermi level is near Dirac points and the energy spectrum has a rotational symmetry in the momentum space. Therefore, it is reasonable to assume that the average $\langle\hat{\Theta}_{\mathbf{p}}\rangle$ is independent of the direction of $\mathbf{p}$. Now, comparing the latter two equations and changing the summation over momentum by integration over energy, we derive the self-consistency equation in the form

$$(\bar{V}_+^2-\bar{V}_-^2)\hat{Q}h(\hat{Q}^\dagger\hat{Q}) = \bar{V}_+\hat{Q} - \bar{V}_-\hat{Q}^\dagger, \tag{61}$$

in which the function h is defined as

$$h(\hat{Q}^\dagger\hat{Q}) = \frac{1}{2}\int_0^{3t}\frac{\nu(\varepsilon)d\varepsilon}{\sqrt{(\varepsilon-t_0)^2+\hat{Q}^\dagger\hat{Q}}}, \tag{62}$$

where $\nu(\varepsilon) \approx \varepsilon/(\sqrt{3}\pi t^2)$ is the graphene density of states (per spin projection per valley) and integration is performed up to maximum electron energy in the AA-BLG [22].

Now we briefly discuss certain mathematical points that must be settled before analysis of the derived equations. Note a property of Eq. (61): if $\hat{Q}_0$ is a solution of this equation, then $\hat{Z}^\dagger\hat{Q}_0\hat{Z}$, where $\hat{Z}$ is a unitary matrix, is also a solution. Observe that the radical of the matrix-valued polynomial in Eqs. (60) and (62) is defined completely unambiguously. Indeed, the

matrix $\hat{Q}^\dagger\hat{Q}$ is Hermitian positive semidefinite (that is, its eigenvalues are real and non-negative). Such a matrix allows the following representation:

$$\hat{Q}^\dagger\hat{Q} = \hat{V}\hat{D}^2\hat{V}^\dagger, \quad \hat{D} = \mathrm{diag}(d_1, \ldots, d_4),\ d_i \geqslant 0 \tag{63}$$

where $\hat{V}$ is a unitary matrix, $\hat{V} \in \mathrm{U}(4)$. Consequently,

$$\left(\varepsilon_{\mathbf{k}}^2 + \hat{Q}^\dagger\hat{Q}\right)^{-\frac{1}{2}} = \hat{V}\left(\varepsilon_{\mathbf{k}}^2 + \hat{D}^2\right)^{-\frac{1}{2}}\hat{V}^\dagger. \tag{64}$$

An arbitrary function f of a diagonal matrix is defined according to the convention

$$f(\mathrm{diag}[a_1, \ldots, a_n]) = \mathrm{diag}[f(a_1), \ldots, f(a_n)], \tag{65}$$

assuming, of course, that $f(a_i)$ are defined for all i's. Applying this construction to Eq. (64) we can write

$$\left(\varepsilon_{\mathbf{k}}^2 + \hat{D}^2\right)^{-\frac{1}{2}} = \mathrm{diag}\left[\left(\varepsilon_{\mathbf{k}}^2 + d_1^2\right)^{-\frac{1}{2}}, \ldots, \left(\varepsilon_{\mathbf{k}}^2 + d_4^2\right)^{-\frac{1}{2}}\right], \tag{66}$$

where the square-root extraction is performed on real non-negative quantities only.

The self-consistency equation (61) can be simplified, if we implement the singular-value decomposition on $\hat{Q}$ and $\hat{Q}^\dagger$:

$$\hat{Q} = \hat{U}\hat{D}\hat{V}^\dagger, \quad \hat{Q}^\dagger = \hat{V}\hat{D}\hat{U}^\dagger, \tag{67}$$

with matrices $\hat{V}$ and $\hat{D}$ being introduced in Eq. (63). As for $\hat{U} \in \mathrm{U}(4)$, it diagonalizes the product $\hat{Q}\hat{Q}^\dagger$, that is, $\hat{Q}\hat{Q}^\dagger = \hat{U}\hat{D}^2\hat{U}^\dagger$. We substitute Eqs. (67) in Eq. (61) and derive a diagonal form of the self-consistency equation

$$[\bar{V}_+ - (\bar{V}_+^2 - \bar{V}_-^2)h(\hat{D}^2)]\hat{D} = \bar{V}_-\hat{W}\hat{D}\hat{W}, \tag{68}$$

where $\hat{W} = \hat{U}^\dagger\hat{V} \in \mathrm{U}(4)$.

Let us assume that we solve the diagonalized self-consistency Eq. (68), that is, we obtain all possible pairs of the matrices $\hat{D}_n$ and $\hat{W}_n$ satisfying Eq. (68). Then, we define

$$\hat{Q}_n = \hat{W}_n^\dagger\hat{D}_n, \quad \hat{Q}_n^\dagger = \hat{D}_n\hat{W}_n. \tag{69}$$

Direct substitution of Eqs. (69) in Eq. (61) shows that $\hat{Q}_n$ is its solution. As it was stated above, all other solutions to the general self-consistency Eq. (61) are unitary equivalent to matrices $\hat{Q}_n$ defined by Eq. (69).

IV. SOLUTIONS OF THE SELF-CONSISTENCY EQUATION

A. The case of vanishing $\bar{V}_-$

First, we consider a simplest case when $\bar{V}_- = 0$. This condition is not realistic but allows one to easily obtain an analytical result. In so doing, Eq. (68) can be rewritten in the BCS-like form

$$1 = \nu_0\bar{V}_+ \ln\left(\frac{2E^*}{\hat{D}}\right), \tag{70}$$

where $\nu_0 \approx t_0/(\sqrt{3}\pi t^2)$ is the AA-BLG density of states at the Fermi level (per spin projection, per valley, per single band), the energy scale is $E^* = \sqrt{t_0(3t - t_0)}$. The solution to this equation reads as

$$\hat{D} = \Delta_0\mathbb{I}_4, \quad \text{where} \quad \Delta_0 = 2E^* \exp\left[-\frac{1}{\nu_0\bar{V}_+}\right], \tag{71}$$

and $\mathbb{I}_4$ is the 4×4 identity matrix. At the same time, when $\bar{V}_-$ vanishes, the matrix $\hat{W}$ is not limited by the self-consistency equation. Lack of any restrictions on $\hat{W}$ is the manifestation of the extended symmetry group G_0 of the model Hamiltonian in the case $\bar{V}_- = 0$. As a result, the order-parameter matrix is $\hat{Q} = \Delta_0\hat{Y}$, where $\hat{Y}$ is an arbitrary unitary matrix. Note that four eigenvalues of $\hat{Q}$ are equal to $\Delta_0 \exp(i\alpha_{1,\ldots,4})$, where α_i are arbitrary phases.

B. Hermitian order parameters

In a general case $V_\pm \neq 0$, the equation system (68) becomes much more complex. Now $\hat{W}$ explicitly enters the self-consistency condition, drastically increasing the number of unknown variables. In this paper we do not attempt to find exhaustive solution to the problem. Instead, we will discuss three specific classes of the solutions of Eq. (68) to illustrate the richness of the system under study.

It is natural to expect that in the ground state of our model the single-electron gaps in the four fermionic sectors are identical to each other. This situation can be represented by the ansatz

$$\hat{D} = \Delta\mathbb{I}_4. \tag{72}$$

Substituting this into Eq. (68), one establishes that

$$\hat{W}^2 = a\mathbb{I}_4, \quad \text{where} \quad a = \pm 1. \tag{73}$$

Let us consider first $a = +1$. Then

$$(\bar{V}_+ + \bar{V}_-)h(\Delta^2) = 1, \quad \hat{W}^2 = \mathbb{I}_4. \tag{74}$$

The solution for Δ is

$$\Delta = 2E^* \exp\left[-\frac{1}{\nu_0(\bar{V}_+ + \bar{V}_-)}\right]. \tag{75}$$

A unitary matrix $\hat{W}$, whose square is $\mathbb{I}_4$, can be expressed as $\hat{W} = \hat{S}\hat{\mathbf{\Sigma}}\hat{S}^\dagger$, where $\hat{S}$ is a unitary matrix, and $\hat{\mathbf{\Sigma}}$ is a diagonal matrix whose elements are ± 1. In such a case, the order-parameter matrix is Hermitian and satisfies

$$\hat{Q} = \hat{Q}^\dagger = \Delta\hat{Z}\hat{\mathbf{\Sigma}}\hat{Z}^\dagger, \tag{76}$$

where $\hat{Z} \in \mathrm{SU}(4)$. In other words, the order parameter is equal to $\Delta\hat{\mathbf{\Sigma}}$ up to a unitary transformation.

To classify all types of $\hat{Q}$ consistent with Eq. (76), we split all possible solutions into three topologically distinct classes labeled by $\alpha \in \{\mathrm{I}, \mathrm{II}, \mathrm{III}\}$. These classes are defined by the structure of $\hat{\mathbf{\Sigma}}$:

$$\text{Class I:} \quad \hat{\mathbf{\Sigma}}_{\mathrm{I}}^\kappa = \mathrm{diag}\,(\kappa, \kappa, \kappa, \kappa),\ \kappa = \pm 1, \tag{77}$$

$$\text{Class II:} \quad \hat{\mathbf{\Sigma}}_{\mathrm{II}} = \mathrm{diag}\,(1, 1, -1, -1), \tag{78}$$

$$\text{Class III:} \quad \hat{\mathbf{\Sigma}}_{\mathrm{III}}^\kappa = \mathrm{diag}\,(\kappa, \kappa, \kappa, -\kappa),\ \kappa = \pm 1. \tag{79}$$

Any $\hat{Q}$ satisfying condition (76) belongs to one and only one class among these three.

Class-I order parameter is a charge-density wave state (CDW). To demonstrate this let us first observe that $\hat{\mathbf{\Sigma}}_{\mathrm{I}}^\kappa \propto \mathbb{I}_4$ and the order parameter is independent of $\hat{Z}$. Thus, it always satisfies $\hat{Q} = \hat{Q}^\dagger = \kappa\Delta\mathbb{I}_4$ and $\hat{Q}$ is diagonal in the multi-index $m = (\xi, \sigma)$ space. Consequently, when calculating local occupation numbers $n_{la} = \sum_\sigma \langle \hat{d}_{\mathbf{n}la\sigma}^\dagger \hat{d}_{\mathbf{n}la\sigma} \rangle$, only "diagonal"

symmetry-breaking averages $\langle\hat{\gamma}^\dagger_{\mathbf{q}3\xi\sigma}\hat{\gamma}_{\mathbf{q}2\xi\sigma}\rangle$ are nonzero. Keeping this in mind and using Eqs. (19) and (20), we derive

$$n_{la} = 1 + \sum_m \delta n_{lam}, \tag{80}$$

where the anomalous contributions to n_{la} are

$$\delta n_{lam} = \frac{(-1)^{a+l}}{2N_c}\sum_{\mathbf{q}} \mathrm{Re}\,\langle\hat{\gamma}^\dagger_{\mathbf{q}3m}\hat{\gamma}_{\mathbf{q}2m}\rangle. \tag{81}$$

These two relations can be compactly written as

$$n_{la} = 1 + \frac{(-1)^{a+l}}{2N_c}\mathrm{Tr}\sum_{\mathbf{q}} \mathrm{Re}\,\langle\hat{\Theta}_{\mathbf{q}}\rangle. \tag{82}$$

Equation (59) allows us to connect $\sum_{\mathbf{q}}\langle\hat{\Theta}_{\mathbf{q}}\rangle$ with $\hat{Q}$, and finally we obtain

$$n_{la} = 1 + \kappa(-1)^{a+l}\frac{2\Delta}{\bar{V}_+ + \bar{V}_-}. \tag{83}$$

Thus, the electric charge distribution is inhomogeneous within a single unit cell, the strength of the inhomogeneity is proportional to Δ. This corresponds to a commensurate CDW state.

The commensurate order parameter does not violate the translation symmetry of the underlying honeycomb lattice. However, the symmetry between the sublattices is broken, and the same is true for the symmetry between the layers. Analyzing Eq. (83) we note that switching layers or sublattices is equivalent to switching the sign of κ. Thus, the inversion of κ is associated with the $\mathbb{Z}_2$ subgroup of the symmetry group G.

Class II contains six mutually unitary-equivalent diagonal matrices $\hat{Q}$. These are $\pm\hat{\mathbf{\Sigma}}_{\mathrm{II}}$ and

$$\pm\mathrm{diag}\,(1,-1,1,-1) \quad \text{and} \quad \pm\,\mathrm{diag}\,(1,-1,-1,1). \tag{84}$$

Any such matrix can be obtained from $\hat{\mathbf{\Sigma}}_{\mathrm{II}}$ by a suitable permutation of its diagonal elements.

If the matrix order parameter $\hat{Q}$ of the class II is diagonal, then, we derive similar to Eq. (81)

$$|\delta n_{lam}| = \frac{\Delta}{2(\bar{V}_+ + \bar{V}_-)}. \tag{85}$$

For fixed l and a, two of δn_{lam} are positive, while two are negative. Thus, unlike the class-I CDW, electronic phases of class II have a homogeneous charge distribution within a unit cell since $\sum_m \delta n_{lam} \equiv 0$ for any l and a. Depending on which δn_{lam}'s are positive, and which are negative, three distinct types of the order can be distinguished: spin-density wave (SDW), valley-density wave (VDW), and spin-valley-density wave (SVDW). For example, the choice

$$\delta n_{la\xi\sigma} = \pm\sigma(-1)^{a+l}|\delta n_{la\xi\sigma}| \tag{86}$$

corresponds to the SDW phase in which the expectation value of the spin operator $\hat{S}^z_{la}$ is finite

$$\langle\hat{S}^z_{la}\rangle = \sum_{\xi\sigma}\sigma\,\delta n_{la\xi\sigma} = \pm(-1)^{a+l}\frac{2\Delta}{\bar{V}_+ + \bar{V}_-}. \tag{87}$$

When $\delta n_{la\xi\sigma} \propto (-1)^\xi$, the system is in the VDW phase, with finite staggered valley polarization

$$\langle\hat{S}^v_{la}\rangle = \sum_{\xi\sigma}(-1)^\xi\delta n_{la\xi\sigma} = \pm(-1)^{a+l}\frac{2\Delta}{\bar{V}_+ + \bar{V}_-}. \tag{88}$$

Finally, the SVDW order corresponds to $\delta n_{la\xi\sigma} \propto (-1)^\xi\sigma$. This phase has finite staggered spin-valley polarization $\langle\hat{S}^{sv}_{la}\rangle = \sum_{\xi\sigma}(-1)^\xi\sigma\,\delta n_{la\xi\sigma}$.

While the class-I order parameter is always the same for any $\hat{Z}$, the class-II matrix $\hat{Q}$ changes when $\hat{Z}$ in Eq. (76) is changed. For example, a suitably chosen $\hat{Z}$ connects all three class-II phases to each other.

Furthermore, in class II, matrix $\hat{Q}$ does not have to be diagonal: for a generic choice of $\hat{Z}$, nonzero elements connecting different spin projections and different valleys are possible. Recall that, if an order parameter is nondiagonal in spin indices, it represents spin polarization deviating from the z axis. Additionally, $\hat{Q}$ can be nondiagonal in valley indices. In real space, these intervalley matrix elements correspond to spatially oscillating contributions, with $\mathbf{K}_1 - \mathbf{K}_2$ being their wave vector. When such an intervalley coherence is realized, the elementary translation vectors are tripled in length.

In *class III*, the diagonal order parameter $\hat{Q} \propto \hat{\mathbf{\Sigma}}^\kappa_{\mathrm{III}}$ represents a state with finite polarizations with respect to all four types of density waves (CDW, SDW, VDW, and SVDW). Unitary matrix $\hat{Z}$ affects the SDW, VDW, and SVDW polarizations. The sign of the CDW order parameter can be changed only by the inversion of κ. The intervalley coherence is also possible in this class.

Finally, we would like to note that in the considered case the order-parameter eigenvalues are always real and equal to $\pm\Delta$ since any Hermitian solution $\hat{Q}$ discussed above is unitary equivalent to $\Delta\hat{\mathbf{\Sigma}}$.

C. Anti-Hermitian order parameters

The order-parameter matrix $\hat{Q}$ does not always have to be Hermitian. To illustrate this point, let us choose $a = -1$ in Eq. (73). In this case we have

$$\hat{W} = i\hat{S}\hat{\mathbf{\Sigma}}\hat{S}^\dagger, \tag{89}$$

where the structures of the matrices $\hat{S}$ and $\hat{\mathbf{\Sigma}}$ are defined in the previous subsection. Assuming that $\hat{D} \propto \mathbb{I}_4$ as in Eq. (72), we substitute this $\hat{W}$ in Eq. (68) and obtain four identical mutually decoupled equations. Solving these equations, we derive

$$\hat{D} = \tilde{\Delta}\mathbb{I}_4, \quad \text{where} \quad \tilde{\Delta} = 2E^*\exp\left[-\frac{1}{\nu_0(\bar{V}_+ - \bar{V}_-)}\right]. \tag{90}$$

The sign before $\bar{V}_-$ is the only difference between Δ and $\tilde{\Delta}$. The order-parameter matrix now reads as

$$\hat{Q} = -\hat{Q}^\dagger = -i\tilde{\Delta}\hat{Z}\hat{\mathbf{\Sigma}}\hat{Z}^\dagger, \tag{91}$$

where $\hat{Z} \in \mathrm{SU}(4)$. Thus, the matrix $\hat{Q}$ is anti-Hermitian.

Following the logic of Sec. IV B, let us consider a special case of $\hat{\Sigma} = \chi\mathbb{I}_4$, where $\chi = \pm 1$. From Eqs. (59) and (91) we obtain that

$$\frac{1}{N_c}\sum_{\mathbf{p}}\langle\hat{\Theta}_{\mathbf{p}}\rangle = -\frac{1}{N_c}\sum_{\mathbf{p}}\langle\hat{\Theta}^\dagger_{\mathbf{p}}\rangle = -\frac{i\chi\tilde{\Delta}}{\bar{V}_+ - \bar{V}_-}. \tag{92}$$

Since $\frac{1}{N_c}\sum_{\mathbf{p}}\langle\hat{\Theta}_{\mathbf{p}}\rangle$ is purely imaginary, then $\delta n_{lam}=0$. On the other hand, "interlayer" current operator

$$\hat{I}^{\perp}_{\mathbf{n}a}=i\sum_{\sigma}\hat{d}^{\dagger}_{\mathbf{n}1a\sigma}\hat{d}_{\mathbf{n}2a\sigma}+\text{H.c.} \tag{93}$$

has a finite expectation value. Let us prove it.

The expectation value $\langle\hat{I}^{\perp}_{\mathbf{n}a}\rangle$ can be presented as a sum over the multi-index m

$$\langle\hat{I}^{\perp}_{\mathbf{n}a}\rangle=\sum_{m}\langle\hat{I}^{\perp}_{am}\rangle, \tag{94}$$

where we assumed that the average $\langle\hat{I}^{\perp}_{\mathbf{n}a}\rangle$ is independent of $\mathbf{n}$ due to ground-state translation invariance. The partial current $\langle\hat{I}^{\perp}_{am}\rangle$ is equal to

$$\langle\hat{I}^{\perp}_{am}\rangle=\frac{1}{2N_c}\sum_{\mathbf{k}}\text{Im}\langle[\hat{\gamma}^{\dagger}_{\mathbf{k}2m}+(-1)^a\hat{\gamma}^{\dagger}_{\mathbf{k}3m}]$$

$$\times[\hat{\gamma}_{\mathbf{k}2m}-(-1)^a\hat{\gamma}_{\mathbf{k}3m}]\rangle.$$

Combining the latter equation and Eq. (92), one derives

$$\langle\hat{I}^{\perp}_{am}\rangle=\frac{(-1)^a}{N_c}\sum_{\mathbf{k}}\text{Im}\langle\hat{\gamma}^{\dagger}_{\mathbf{k}3m}\hat{\gamma}_{\mathbf{k}2m}\rangle=\frac{\chi(-1)^a\tilde{\Delta}}{\bar{V}_+-\bar{V}_-}. \tag{95}$$

Consequently,

$$\langle\hat{I}^{\perp}_{\mathbf{n}a}\rangle=\chi(-1)^a\frac{4\tilde{\Delta}}{\bar{V}_+-\bar{V}_-}. \tag{96}$$

We see that such a state is characterized by spontaneously generated interlayer currents. Factor $(-1)^a$ in the expression for $\langle\hat{I}^{\perp}_{\mathbf{n}a}\rangle$ indicates that the flow along the interlayer links on sublattice A exactly cancels the flow along the interlayer links on sublattice B. Therefore, the overall interlayer charge flow is zero, as it must be in an eigenstate. Note also, a detailed distribution of the current flow is impossible to calculate within the current formalism since we neglect the existence of the bands 1 and 4.

One can adopt the reasoning of Sec. IV B and introduce a topological classification of the anti-Hermitian order parameters: there are three distinct classes, whose order parameters are identical, up to multiplication on complex unity i, to the order parameters in classes I, II, and III discussed above. Instead of the spontaneous local densities, the ordered states corresponding to the anti-Hermitian $\hat{Q}$ are characterized by spontaneous interlayer currents. Depending on the topological class, these currents may carry charge, spin, valley, spin-valley quanta, or combinations of the above.

D. Non-Hermitian non-anti-Hermitian order parameters

In this section we demonstrate that the order parameter $\hat{Q}$ satisfying the self-consistency equation (61) may be neither Hermitian nor anti-Hermitian. To prove this point, let us consider the matrix set $\mathfrak{M}$ that contains 4^4 diagonal matrices of the following structure:

$$\hat{W}=\text{diag}\,(w_1,\ldots,w_4),\quad\text{where}\quad w_m=\pm1,\pm i. \tag{97}$$

Any diagonal matrix that satisfies condition (73) unavoidably satisfies Eq. (97). Therefore, all matrices $\hat{W}$ discussed in Secs. IV B and IV C belong to the set $\mathfrak{M}$. The inverse statement is obviously not true.

The matrices that belong to $\mathfrak{M}$ but violate condition (73) can be described in terms of their diagonal elements (up to a permutation) as follows:

$$w_1=\pm1,\quad w_2=\pm1,\pm i,\quad w_3=\pm1,\pm i,\quad w_4=\pm i. \tag{98}$$

For matrices $\hat{W}$ of this type the self-consistency condition splits into four decoupled equations. However, not all of these equations are identical. It is easy to demonstrate that the diagonal elements of $\hat{D}$ satisfy

$$d_m=\begin{cases}\Delta, & \text{if}\quad w_m=\pm1\\ \tilde{\Delta}, & \text{if}\quad w_m=\pm i.\end{cases} \tag{99}$$

Diagonal order parameter $\hat{Q}^{\dagger}$ equals

$$\hat{Q}^{\dagger}=\text{diag}(w_1d_1,\ldots,w_4d_4). \tag{100}$$

Nondiagonal $\hat{Q}^{\dagger}$ can be obtained by application of a unitary transformation. We clearly see that all such order parameters are neither Hermitian nor anti-Hermitian.

The order parameter (100) represents a state that includes the features of both the Hermitian and the anti-Hermitian order-parameter states. If w_m is real, the nonvanishing symmetry-breaking observable for this multi-index m is the local density $\langle\delta n_{lam}\rangle\neq0$, as in Sec. IV B, otherwise, it is the interlayer current $\langle I^{\perp}_{am}\rangle\neq0$, as in Sec. IV C. Table I presents a classification scheme for these ordered phases.

TABLE I. Classification of non-Hermitian non-anti-Hermitian order parameters. All matrices $\hat{Q}^{\dagger}$ described by Eq. (100) can be split into three types according to the number of real eigenvalues. Each column of the table represents one of these types. We use the following notations: ±1 stands for a real eigenvalue, $\pm i$ stands for an imaginary eigenvalue, and the binary indices $\kappa=\pm1$ and $\chi=\pm1$ are the same as in Secs. IV B and IV C. Within each type, additional subtypes can be defined, according to the number of minus signs in front of real and imaginary eigenvalues (up to a permutation of eigenvalues). Any diagonal order-parameter matrix set by Eq. (100) belongs to one and only one subtype defined in this table.

1 real eigenvalue $(\pm1,\pm i,\pm i,\pm i)$	2 real eigenvalues $(\pm1,\pm1,\pm i,\pm i)$	3 real eigenvalues $(\pm1,\pm1,\pm1,\pm i)$
$(\kappa,i\chi,i\chi,i\chi)$	$(\kappa,\kappa,i\chi,i\chi)$	$(\kappa,\kappa,\kappa,i\chi)$
$(\kappa,i\chi,i,-i)$	$(\kappa,\kappa,i,-i)$	$(\kappa,1,-1,i\chi)$
	$(1,-1,i\chi,i\chi)$	
	$(1,-1,i,-i)$	

V. DISCUSSION

Due to peculiar features of the honeycomb lattice, the single-electron dispersion in graphene and graphene-based systems is characterized by an additional quantum number, valley index. Although, in many respects, the valley index differs from the spin projection, it is possible to formulate a theory that incorporates these two quantum numbers on an equal footing. Our paper presents such a theory for the specific case of AA-BLG.

An SU(4)-symmetric [SU(4)S] theory of a graphene-based system cannot serve as an ultimate model describing electronic properties in detail. Yet, it is a helpful theoretical tool. Let us recall that the presence of the valley degeneracy in graphene-based materials opens new possibilities for

electron-electron scattering and electron low-temperature ordering. In such a situation, an accurate "bookkeeping" of all scattering and ordering channels may be quite challenging. A study of an SU(4)S model should be viewed as a physically motivated approach aiming at developing a concise classification scheme of the ordered states in graphene-based materials.

The discussion presented above attests both to difficulties that one faces when trying to itemize all allowed ordered phases in AA-BLG, and to usefulness of an SU(4)S model for such an endeavor. Our main result here is the derivation of the self-consistency Eq. (68) and the list (possibly, incomplete) of ordered phases satisfying this equation. One should appreciate the length of this list, as well as the fact that all these dissimilar many-body states have been identified within a single unifying approach, as solutions to Eq. (68).

At the same time, the proposed method suffers from several limitations that require additional research. One must remember that a single state with lowest energy inevitably becomes the true ground state. Trying to use the SU(4)S model to determine which state is the ground state, we discover that quite dissimilar phases aggregate into broad multiplicities, with all phases in a multiplicity being degenerate and connected to each other by suitable SU(4) Bogolyubov transformations. For example, class II of the Hermitian ordered phases unites SDW, VDW, and SVDW into a single group of degenerate states. This "blindness" of the classification is a consequence of consideration of the spin and valley indices on an equal footing.

Clearly, a more realistic theory must distinguish the valley quantum, of purely orbital origin, and spin, a consequence of the relativistic Dirac-equation physics. In a general situation one expects that non-SU(4)S terms in the Hamiltonian destroy the spin-valley symmetry, and lift multiple degeneracies of the SU(4)S model. In this respect, we already identified the backscattering interaction as a non-SU(4)S term. Other possible non-SU(4)S contributions may emerge when electron-lattice coupling is taken into account. The short-range interaction is also incompatible with the SU(4)S. Additionally, external influences (electric and/or magnetic fields, substrate choice, deformations, etc.) engineered for a specific purpose (e.g., stabilizing a specific type of order parameter) must be considered as well.

Under such circumstances, we expect that the true ground state will be chosen from the list as a result of the interplay of various nonuniversal and, possibly, sample-specific factors. Situations of this sort, when multiple states compete against each other to become the true ground state, are known to appear in doped Hubbard model [7,9,10], and models with nesting [8,14,15,23–26]. Unlike these, for our SU(4)S model such competition occurs already at zero doping. However, the aspect common for both types of models is the importance of numerous nonuniversal contributions affecting the final outcome of the competition [7].

Two additional questions for the future research are (i) the completeness of the ordered phase list and (ii) the stability of the phases in that list. In connection to (i) we must say that within our formalism this problem becomes a purely mathematical task of exhausting all possible solutions to Eq. (68). Currently, we do not know if ordered states other than those discussed in Sec. IV can be identified.

As for (ii), we want to emphasize that a stability study of an ordered state may be very complicated, and any self-consistency equation is insufficient to establish stability or metastability of its solutions. For a mean field theory, like ours, one can compare mean field energies for various states. For example, it is easy to show that, for positive $\bar{V}_+$, the Hermitian order-parameter state has lower energy than the anti-Hermitian when $\bar{V}_- > 0$. For negative $\bar{V}_-$, the anti-Hermitian order-parameter states have lower mean field energy. For any sign of $\bar{V}_-$, the order parameter (100) has the energy that is in-between the two.

The latter argumentation, however, ignores the issue of the non-mean-field fluctuations. They are important for two reasons: the fluctuation-induced contributions to the energy can potentially lift the degeneracies between different multiplicities [21], and the fluctuations can completely destroy the order through the Mermin-Wagner-Hohenberg mechanism. These two problems are the two sides to the same looming question: the reliability of the mean field theory. While, at present, it is impossible to address this question in full generality, a good measure of theoretical understanding is already available. For AA-BLG and other two-dimensional systems, it is expected that the mean field theory is valid at zero temperature, at least qualitatively. Zero-temperature fluctuation corrections to the mean field energy may be of the same order as the mean field energy itself [21]. This does present a certain theoretical difficulty [27]. Fortunately, these corrections often can be interpreted [7,27] as (weak) renormalizations to the interaction constants, which allows one to preserve the general mean field structure of the theory.

As for Mermin-Wagner-Hohenberg mechanism, it is well recognized that any non-Ising order in a two-dimensional system cannot endure finite temperatures. Yet, the destroyed order does not disappear completely, but rather survives in the form of short-range correlations, which gradually vanish through a crossover. For a specific case of the SDW in AA-BLG, qualitative theory of this crossover was discussed in Ref. [15].

As we noted in Sec. I, our analysis of the order-parameter symmetries in the AA-BLG is an extension of the approach proposed by Nandkishore and Levitov in Ref. [21] for AB-BLG. However, the authors of Ref. [21] limited themselves by the study of Hermitian order parameters only. We guess that including in the consideration non-Hermitian orders in the AB-BLG is of interest and can be performed using the present approach. Of a particular interest is the study of the order parameters in twisted bilayer graphene. At low-twist angles (and at magical angles, in particular), this system can be considered as a periodic arrangement of regions with AA and AB stacking. Thus, the analysis of the possible symmetries of the order parameters in "aligned" bilayers (AB-BLG and AA-BLG) can be considered as a first step for study of the twisted graphene systems.

Finally, we want to mention that the proposed approach may be useful for classification of superconducting order parameters in graphene-based systems. However, in this case the consideration requires a significant modification. In particular, we should take into account effects of doping. So, the analysis of the superconducting orders is beyond the scope of this work and is the topic of further studies.

To conclude, we present a SU(4)-invariant model for the AA-BLG and investigate this model within the mean field approximation. The derived matrix self-consistency equation demonstrates rich diversity of solutions, every solution representing a stationary ordered many-body phase of our model. This wealth of the ordered states with close energies indicates that in the AA-BLG several ordered phases compete against each other to become the true ground state. Symmetry-based classification of the discussed phases is developed.

ACKNOWLEDGMENT

This research was funded by Russian Science Foundation Grant No. 22-22-00464.

APPENDIX: CALCULATION OF THE SYMMETRY-BREAKING AVERAGE

To derive the self-consistency relation in the form of Eq. (60) we need to express $N_c^{-1}\sum_{\mathbf{q}}\langle\hat{\Theta}_{\mathbf{q}}\rangle$ in terms of $\hat{Q}$. A convenient approach to address this task is to use the Hellmann-Feynman formula

$$\left\langle\frac{\partial\hat{H}}{\partial\lambda}\right\rangle=\frac{\partial E_0}{\partial\lambda}, \tag{A1}$$

where $\hat{H}$ is a Hamiltonian dependent on some parameter λ, and $E_0=E_0(\lambda)$ is the ground-state energy of $\hat{H}(\lambda)$.

To adopt the latter formula to our mean field approximation, we need to look for extrema of $E^{\mathrm{MF}}=E^{\mathrm{MF}}(\hat{Q},\hat{Q}^\dagger)$ over $\hat{Q}$. Since $\hat{Q}$ is a matrix, it is useful to introduce the differentiation over a matrix. Namely, the derivative $\frac{\partial f(\hat{X})}{\partial\hat{X}}$ is a matrix $\hat{Y}=\frac{\partial f}{\partial\hat{X}}$ whose elements $y_{ss'}$ are equal to

$$y_{ss'}=\frac{\partial f}{\partial x_{s's}}, \tag{A2}$$

where $x_{ss'}$ are elements of $\hat{X}$. This definition implies that

$$\frac{\partial}{\partial\hat{X}}\mathrm{Tr}(\hat{A}\hat{X})=\hat{A}, \tag{A3}$$

provided that $\hat{A}$ itself is independent of $\hat{X}$. Using these notations and the theorem (A1), we obtain for our mean field Hamiltonian (56)

$$\frac{1}{N_c}\sum_{\mathbf{q}}\langle\hat{\Theta}_{\mathbf{q}}\rangle=-\frac{\partial E^{\mathrm{MF}}}{\partial\hat{Q}^\dagger}, \tag{A4}$$

$$\frac{1}{N_c}\sum_{\mathbf{q}}\langle\hat{\Theta}^\dagger_{\mathbf{q}}\rangle=-\frac{\partial E^{\mathrm{MF}}}{\partial\hat{Q}}, \tag{A5}$$

where E^{MF} is the ground-state energy (per unit cell) for $\hat{H}^{\mathrm{MF}}$ [see Eq. (57)].

To calculate E^{MF} it is convenient to write $\hat{H}^{\mathrm{MF}}$ [Eq. (56)] as follows:

$$\hat{H}^{\mathrm{MF}}=\sum_{\mathbf{q}}\Phi^\dagger_{\mathbf{q}}\hat{\mathcal{H}}_{\mathbf{q}}\Phi_{\mathbf{q}}. \tag{A6}$$

In this formula the eight-component vector $\Phi^\dagger_{\mathbf{q}}$ equals

$$\Phi^\dagger_{\mathbf{q}}=(\Psi^\dagger_{\mathbf{q}2},\Psi^\dagger_{\mathbf{q}3}), \tag{A7}$$

where band-specific vectors $\Psi^\dagger_{\mathbf{q}s}$ ($s=2,3$) are introduced according to

$$\Psi^\dagger_{\mathbf{q}s}=(\hat{\gamma}^\dagger_{\mathbf{q}s\uparrow\mathbf{K}_1},\hat{\gamma}^\dagger_{\mathbf{q}s\downarrow\mathbf{K}_1},\hat{\gamma}^\dagger_{\mathbf{q}s\uparrow\mathbf{K}_2},\hat{\gamma}^\dagger_{\mathbf{q}s\downarrow\mathbf{K}_2}). \tag{A8}$$

Symbol $\hat{\mathcal{H}}_{\mathbf{q}}$ in Eq. (A6) is the 8×8 matrix defined as

$$\hat{\mathcal{H}}_{\mathbf{q}}=\begin{pmatrix}\varepsilon_{\mathbf{q}}\mathbb{I}_4 & -\hat{Q}^{\mathrm{T}}\\ -\hat{Q}^* & -\varepsilon_{\mathbf{q}}\mathbb{I}_4\end{pmatrix}, \tag{A9}$$

where $\varepsilon_{\mathbf{q}}=v_{\mathrm{F}}|\mathbf{q}|-t_0$.

The energy E^{MF} then equals

$$E^{\mathrm{MF}}=\frac{1}{N_c}\sum_{\mathbf{q}}\sum_{n=1,\ldots,8}\mathcal{E}^{(n)}_{\mathbf{q}}\vartheta\left(-\mathcal{E}^{(n)}_{\mathbf{q}}\right), \tag{A10}$$

where $\vartheta(x)$ is the step function, and $\mathcal{E}^{(n)}_{\mathbf{q}}$ is the nth eigenvalue of $\hat{\mathcal{H}}_{\mathbf{q}}$. Thus, we need to calculate the eigenvalues of $\hat{\mathcal{H}}_{\mathbf{q}}$. It is more convenient to replace the matrix $\hat{\mathcal{H}}_{\mathbf{q}}$ with its complex conjugate $\hat{\mathcal{H}}^*_{\mathbf{q}}$, which, however, has the same set of $\mathcal{E}^{(n)}_{\mathbf{q}}$. The eigenvalue-eigenvector relation for $\hat{\mathcal{H}}^*_{\mathbf{q}}$ reads as

$$\begin{pmatrix}\varepsilon_{\mathbf{q}} & -\hat{Q}^\dagger\\ -\hat{Q} & -\varepsilon_{\mathbf{q}}\end{pmatrix}\begin{pmatrix}\phi_1\\ \phi_2\end{pmatrix}=\mathcal{E}_{\mathbf{q}}\begin{pmatrix}\phi_1\\ \phi_2\end{pmatrix}. \tag{A11}$$

Excluding ϕ_2 from this equation, we derive

$$\left(\mathcal{E}^2_{\mathbf{q}}-\varepsilon^2_{\mathbf{q}}\right)\phi_1=\hat{Q}^\dagger\hat{Q}\phi_1. \tag{A12}$$

Thus, the eigenenergies of $\hat{\mathcal{H}}_{\mathbf{q}}$ are

$$\mathcal{E}^{(n)}_{\mathbf{q}}=\pm\sqrt{\varepsilon^2_{\mathbf{q}}+d_i^2}, \tag{A13}$$

where d_i^2, $i=1,\ldots,4$, are the eigenvalues of the positive-semidefinite 4×4 matrix $\hat{Q}^\dagger\hat{Q}$. Since the trace of a matrix is invariant under unitary transformations, we derive

$$E^{\mathrm{MF}}=-\frac{1}{N_c}\sum_{\mathbf{q}}\mathrm{Tr}\left(\varepsilon^2_{\mathbf{q}}+\hat{Q}^\dagger\hat{Q}\right)^{\frac{1}{2}}. \tag{A14}$$

The final step is to find the derivatives $\partial E^{\mathrm{MF}}/\partial\hat{Q}$ and $\partial E^{\mathrm{MF}}/\partial\hat{Q}^\dagger$. For this goal, we expand Eq. (A14) in powers of $\hat{Q}^\dagger\hat{Q}$. Using definition (A2), we can demonstrate that

$$\frac{\partial}{\partial\hat{Q}^\dagger}\mathrm{Tr}(\hat{Q}^\dagger\hat{Q})^n=n\hat{Q}(\hat{Q}^\dagger\hat{Q})^{n-1}. \tag{A15}$$

We see that the differentiation rule for this monomial is essentially identical to the rule for differentiating a product of commuting variables. Such a simplification occurs due to invariance of the trace under cyclic permutation of multipliers under sign of the trace. This allows us to perform a resummation of the power series and derive

$$-\frac{\partial E^{\mathrm{MF}}}{\partial\hat{Q}^\dagger}=\frac{1}{2N_c}\sum_{\mathbf{q}}\hat{Q}\left(\varepsilon^2_{\mathbf{q}}+\hat{Q}^\dagger\hat{Q}\right)^{-\frac{1}{2}}. \tag{A16}$$

Thus we obtain the self-consistency condition (60). Similarly, one can derive

$$-\frac{\partial E^{\mathrm{MF}}}{\partial\hat{Q}}=\frac{1}{2N_c}\sum_{\mathbf{q}}\left(\varepsilon^2_{\mathbf{q}}+\hat{Q}^\dagger\hat{Q}\right)^{-\frac{1}{2}}\hat{Q}^\dagger, \tag{A17}$$

which can be used in Eq. (A5).

[1] Y. Cao, V. Fatemi, A. Demir, S. Fang, S. L. Tomarken, J. Y. Luo, J. D. Sanchez-Yamagishi, K. Watanabe, T. Taniguchi, E. Kaxiras *et al.*, Correlated insulator behaviour at half-filling in magic-angle graphene superlattices, Nature (London) **556**, 80 (2018).

[2] Y. Cao, V. Fatemi, S. Fang, K. Watanabe, T. Taniguchi, E. Kaxiras, and P. Jarillo-Herrero, Unconventional superconductivity in magic-angle graphene superlattices, Nature (London) **556**, 43 (2018).

[3] X. Lu, P. Stepanov, W. Yang, M. Xie, M. A. Aamir, I. Das, C. Urgell, K. Watanabe, T. Taniguchi, G. Zhang *et al.*, Superconductors, orbital magnets and correlated states in magic-angle bilayer graphene, Nature (London) **574**, 653 (2019).

[4] S. C. de la Barrera, S. Aronson, Z. Zheng, K. Watanabe, T. Taniguchi, Q. Ma, P. Jarillo-Herrero, and R. Ashoori, Cascade of isospin phase transitions in Bernal-stacked bilayer graphene at zero magnetic field, Nat. Phys. **18**, 771 (2022).

[5] H. Zhou, L. Holleis, Y. Saito, L. Cohen, W. Huynh, C. L. Patterson, F. Yang, T. Taniguchi, K. Watanabe, and A. F. Young, Isospin magnetism and spin-polarized superconductivity in Bernal bilayer graphene, Science **375**, 774 (2022).

[6] A. M. Seiler, F. R. Geisenhof, F. Winterer, K. Watanabe, T. Taniguchi, T. Xu, F. Zhang, and R. T. Weitz, Quantum cascade of correlated phases in trigonally warped bilayer graphene, Nature (London) **608**, 298 (2022).

[7] S. V. Kokanova, P. A. Maksimov, A. V. Rozhkov, and A. O. Sboychakov, Competition of spatially inhomogeneous phases in systems with nesting-driven spin-density wave state, Phys. Rev. B **104**, 075110 (2021).

[8] A. O. Sboychakov, A. L. Rakhmanov, A. V. Rozhkov, and F. Nori, Bilayer graphene can become a fractional metal, Phys. Rev. B **103**, L081106 (2021).

[9] P. Corboz, T. M. Rice, and M. Troyer, Competing states in the t-J model: Uniform d-Wave state versus stripe state, Phys. Rev. Lett. **113**, 046402 (2014).

[10] B.-X. Zheng, C.-M. Chung, P. Corboz, G. Ehlers, M.-P. Qin, R. M. Noack, H. Shi, S. R. White, S. Zhang, and G. K.-L. Chan, Stripe order in the underdoped region of the two-dimensional Hubbard model, Science **358**, 1155 (2017).

[11] A. Narayanan, A. Kiswandhi, D. Graf, J. Brooks, and P. Chaikin, Coexistence of spin density waves and superconductivity in $(TMTSF)_2PF_6$, Phys. Rev. Lett. **112**, 146402 (2014).

[12] A. L. Rakhmanov, A. V. Rozhkov, A. O. Sboychakov, and F. Nori, Instabilities of the *AA*-stacked graphene bilayer, Phys. Rev. Lett. **109**, 206801 (2012).

[13] L. Brey and H. A. Fertig, Gapped phase in *AA*-stacked bilayer graphene, Phys. Rev. B **87**, 115411 (2013).

[14] A. O. Sboychakov, A. L. Rakhmanov, A. V. Rozhkov, and F. Nori, Metal-insulator transition and phase separation in doped AA-stacked graphene bilayer, Phys. Rev. B **87**, 121401(R) (2013).

[15] A. O. Sboychakov, A. V. Rozhkov, A. L. Rakhmanov, and F. Nori, Antiferromagnetic states and phase separation in doped AA-stacked graphene bilayers, Phys. Rev. B **88**, 045409 (2013).

[16] R. S. Akzyanov, A. O. Sboychakov, A. V. Rozhkov, A. L. Rakhmanov, and F. Nori, *AA*-stacked bilayer graphene in an applied electric field: Tunable antiferromagnetism and coexisting exciton order parameter, Phys. Rev. B **90**, 155415 (2014).

[17] D. S. de la Peña, M. M. Scherer, and C. Honerkamp, Electronic instabilities of the AA-honeycomb bilayer, Ann. Phys. **526**, 366 (2014).

[18] H. M. Abdullah, M. Al Ezzi, and H. Bahlouli, Electronic transport and Klein tunneling in gapped AA-stacked bilayer graphene, J. Appl. Phys. **124**, 204303 (2018).

[19] A. Laref, M. Alsagri, S. M. Alay-e-Abbas, S. Laref, H. Huang, Y. Xiong, J. Yang, S. A. Khandy, D. P. Rai, D. Varshney *et al.*, Electronic structure and optical characteristics of AA stacked bilayer graphene: A first principles calculations, Optik **206**, 163755 (2020).

[20] V. Apinyan and T. K. Kopeć, Antiferromagnetic ordering and excitonic pairing in AA-stacked bilayer graphene, Phys. Rev. B **104**, 075426 (2021).

[21] R. Nandkishore and L. Levitov, Quantum anomalous Hall state in bilayer graphene, Phys. Rev. B **82**, 115124 (2010).

[22] A. Rozhkov, A. Sboychakov, A. Rakhmanov, and F. Nori, Electronic properties of graphene-based bilayer systems, Phys. Rep. **648**, 1 (2016).

[23] A. V. Rozhkov, A. L. Rakhmanov, A. O. Sboychakov, K. I. Kugel, and F. Nori, Spin-valley half-metal as a prospective material for spin valleytronics, Phys. Rev. Lett. **119**, 107601 (2017).

[24] A. O. Sboychakov, A. V. Rozhkov, K. I. Kugel, A. L. Rakhmanov, and F. Nori, Electronic phase separation in iron pnictides, Phys. Rev. B **88**, 195142 (2013).

[25] A. L. Rakhmanov, A. V. Rozhkov, A. O. Sboychakov, and F. Nori, Phase separation of antiferromagnetic ground states in systems with imperfect nesting, Phys. Rev. B **87**, 075128 (2013).

[26] A. Gorbatsevich, Y. Kopaev, and I. Tokatly, Band theory of phase stratification, Zh. Eksp. Teor. Fiz. **101**, 971 (1992) [JETP **74**, 521 (1992)].

[27] M. Hoyer and J. Schmalian, Role of fluctuations for density-wave instabilities: Failure of the mean-field description, Phys. Rev. B **97**, 224423 (2018).